low[25]. The zinc and the Fe hypotheses may thus explain the low atmospheric CO_2 during the last glacial maximum. □

Received 14 February; accepted 1 June 1994.

1. Raven, J. A. & Johnston, A. M. *Limnol. Oceanogr.* **36,** 1701–1714 (1991).
2. Broecker, W. S. *Globl Biogeochem. Cycles* **5,** 191–192 (1991).
3. Sarmiento, J. L. & Toggweiler, J. R. *Nature* **308,** 621–624 (1984).
4. Riebesell, U., Wolf-Gladrow, D. A. & Smetacek, V. S. *Nature* **361,** 249–251 (1993).
5. Sultemeyer, D. F., Miller, A. G., Espie, G. S., Fock, H. P. & Canvin, D. T. *Pl. Physiol.* **89,** 1213–1219 (1989).
6. Price, G. D. & Badger, M. R. *Pl. Physiol.* **89,** 37–43 (1989).
7. Bruland, K. W. *Limnol. Oceanogr.* **34,** 269–285 (1989).
8. Anderson, M. A., Morel, F. M. M. & Guillard, R. R. L. *Nature* **276,** 70–71 (1978).
9. Sunda, W. G. & Huntsman, S. A. *Limnol. Oceanogr.* **37,** 25–40 (1992).
10. Martin, J. H. & Fitzwater, S. E. *Nature* **331,** 341–343 (1988).
11. Price, N. M. & Morel, F. M. M. *Nature* **344,** 658–660 (1990).
12. Mook, W. G., Bommerson, J. C. & Staverman, W. H. *Earth planet. Sci. Lett.* **22,** 169–176 (1974).
13. Rau, G. H., Takahashi, T., Des Marais, D. J., Repeta, D. J. & Martin, J. H. *Geochim. cosmochim. Acta* **56,** 1413–1419 (1992).
14. Freeman, K. H. & Hayes, J. M. *Globl Biogeochem. Cycles* **6,** 185–198 (1992).
15. Codispoti, L. A., Friederich, G. E., Iverson, R. L. & Hood, D. W. *Nature* **296,** 242–245 (1982).
16. Broecker, W. S. & Peng, T.-H. *Tracers in the Sea* (Eldigio, Palisades, New York, 1982).
17. Bruland, K. W. *Limnol. Oceanogr.* **37,** 1008–1017 (1992).
18. Hudson, R. J. M. & Morel, F. M. M. *Deep-Sea Res.* **40,** 129–150 (1993).
19. Price, N. M., Ahner, B. A. & Morel, F. M. M. *Limnol. Oceanogr.* **39,** 520–534 (1994).
20. Quiroga, O. & Gonzalez, E. L. *J. Phycol.* **29,** 321–324 (1993).
21. Sikes, S. S. & Wheeler, A. P. *J. Phycol.* **18,** 423–426 (1982).
22. Nimer, N. A. & Merrett, M. J. *New Phytol.* **121,** 173–177 (1992).
23. Petit, J. R., Briat, M. & Royer, A. *Nature* **293,** 391–393 (1981).
24. Arimoto, R., Duce, R. A., Ray, B. J., Hewitt, A. B. & Williams, J. *J. geophys. Res.* **92,** 8465–8479 (1987).
25. Pedersen, T. F. *Geology* **11,** 16–19 (1983).
26. Price, N. M. *et al. Biol. Oceanogr.* **6,** 443–461 (1988/89).
27. Graham, D., Reed, M. L., Patterson, B. D. & Hockley, D. G. *Annls N.Y. Acad. Sci.* **429,** 222–237 (1984).

Where we look when we steer

M. F. Land* & D. N. Lee†

* Sussex Centre for Neuroscience, School of Biological Sciences, University of Sussex, Brighton BN1 9QG, UK
† Perception in Action Laboratories, Department of Psychology, University of Edinburgh, 7 George Square, Edinburgh EH8 9JZ, UK

STEERING a car requires visual information from the changing pattern of the road ahead. There are many theories about what features a driver might use[1–3], and recent attempts to engineer self-steering vehicles have sharpened interest in the mechanisms involved[4,5]. However, there is little direct information linking steering performance to the driver's direction of gaze[3]. We have made simultaneous recordings of steering-wheel angle and drivers' gaze direction during a series of drives along a tortuous road. We found that drivers rely particularly on the 'tangent point' on the inside of each curve, seeking this point 1–2 s before each bend and returning to it throughout the bend. The direction of this point relative to the car's heading predicts the curvature of the road ahead, and we examine the way this information is used.

Steering performance was measured using a Jaguar car equipped with instruments to record and store information on the angle of the steering wheel, speed and other parameters. The car had automatic transmission and power steering. Gaze direction was measured using a head-based video system which imaged both the road ahead and the driver's eye[6,7]. A computer

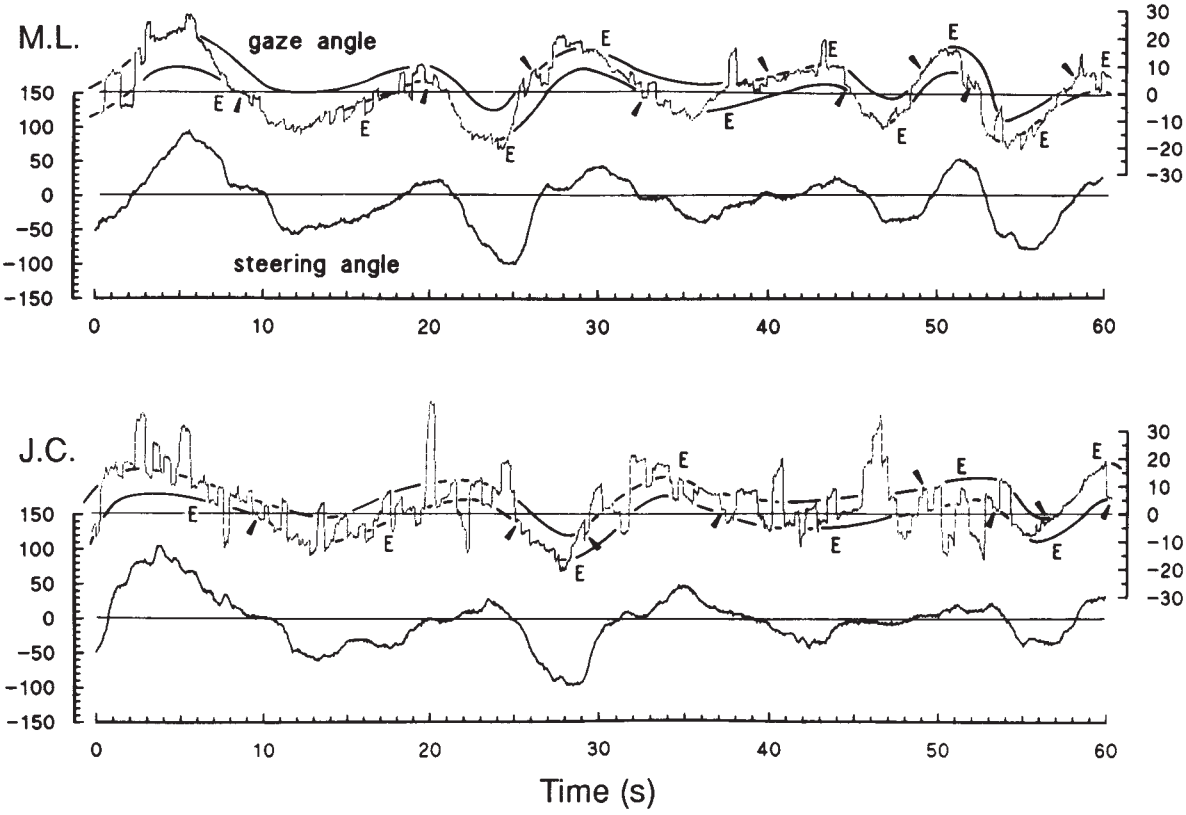

FIG. 1 Simultaneous records of gaze angle relative to the car's heading and steering-wheel angle for two drivers (M.L. and J.C.) driving the same twisting road. M.L. drove slightly faster (45 km h^{-1}) than J.C. (40 km h^{-1}). The performance of a third driver (A.M.) was very similar to M.L.'s. The approximate locations of the edges of the road have been added to the gaze angle traces. This was done by measuring on the video the positions of the sides of the road at the distance at which gaze direction intersected the road (typically 20–30 m). These records show how gaze moves to the right road edge on right-hand bends and to the left road edge on left-hand bends. Arrowheads indicate the first clear saccade to the tangent point preceding each bend, and E is the point on the exit from each bend where the tangent point disappears. J.C. spends more time looking off the road than M.L., but still returns frequently to the tangent points. These may be tracked by repeated refixations (for example, J.C. 9–17 s) or smooth tracking (M.L., 48–51 s, J.C., 56–59 s), or a combination. Records were synchronized to better than 0.1 s by comparing the steering-angle record with steering-wheel movements seen on the gaze video. Both scales are in degrees.

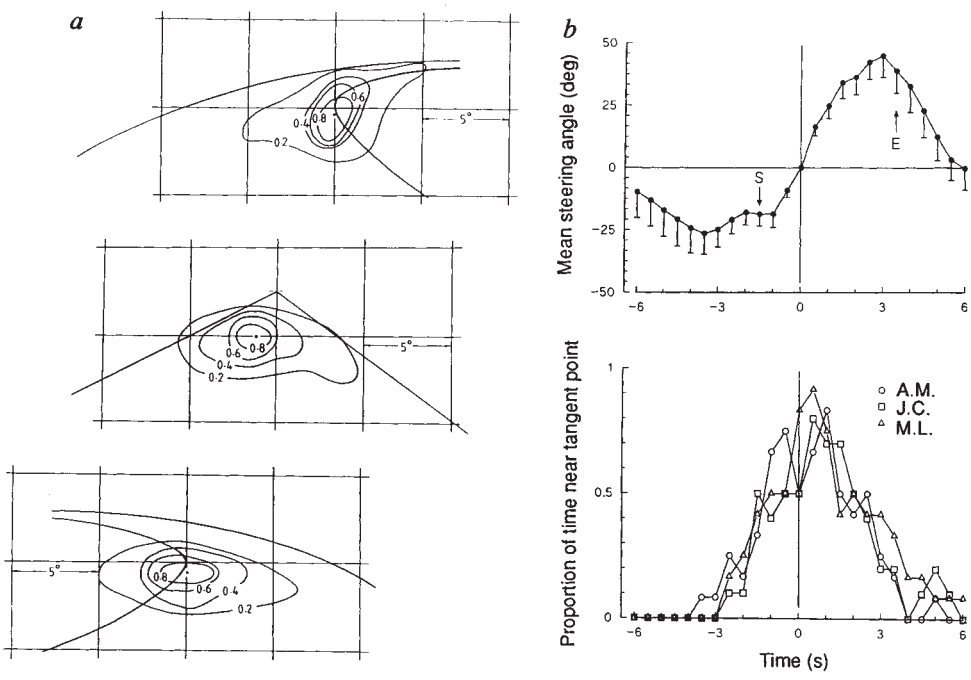

FIG. 2 *a*, Contour plots showing the distribution of the centre points of all fixations made during right bends (top), left bends (bottom) and when no tangent point was visible (centre). Bends are taken to be between the first fixation on the tangent point (arrowheads in Fig. 1, and S in *b*) and the time of its disappearance (*E* in *b*). Through the bends, all measurements were made with respect to the tangent point itself, and on the straight parts with respect to the vanishing point. Contour intervals are proportions of the maximum value, the absolute value of which is ~0.12 fixations per $deg^2 s^{-1}$. About 35% of all fixations lie beyond the 0.2 contour, and are widely spread. Figures have been positioned so that the car's heading is aligned on all three, and corresponds to the centre line in the centre figure. Data from the drivers have been pooled; all three drivers showed very similar distributions on the road itself, although J.C. made relatively more remote fixations. *b*, Time course of the use of the tangent point. Top, steering-wheel angle adopted around a 'typical' bend averaged from the 10 largest bends on the drive, synchronized to the point when the steering wheel angle is zero (0 s on *x*-axis). Bars indicate 1 s.e. Arrow at S shows average timing of the first saccade to tangent point, and *E* the average timing of its disappearance. Bottom, the portion of the total time spent by the gaze of each driver within 3° of the tangent point. It can be seen that during the first second into the turn, all three drivers look at the tangent point almost all (>75%) of the time.

model of the eye was used to convert the recorded position of the iris into direction of view relative to the head, and this was added as a spot to the image of the road. Head movements were monitored from the movement on the video image of a series of markers on the car's windscreen. Eye-in-head and head-in-car coordinates were added to give eye-in-car (gaze) records (Fig. 1). Gaze measurements are repeatable to better than 1°, and the absolute accuracy in the central 20° region is about 1°. Three experienced drivers (J.C., A.M. and M.L.) drove at normal speeds around Arthur's Seat in Edinburgh. This road has many bends, but is single-lane and one way and so provides demanding steering conditions uncomplicated by traffic.

Figure 1 shows 1-min records of steering-wheel angle and gaze direction from two drivers. Both gaze records show a typical pattern of saccades, fixations, and smooth tracking[8]. For driver M.L. steering and gaze records are very similar, with the steering wheel turned at an angle corresponding to the direction of gaze relative to the car's heading, after a delay of about 0.75 s. For driver J.C., this relation is less obvious because he spends more time looking off the road at the scenery but, like driver M.L., he keeps returning his gaze to the sides of the road.

Viewing the videos of all three drivers, one is immediately struck by the way the eye seeks and returns to the 'tangent point' (reversal or extremal point) on the inside of each bend, where the edge of the road reverses direction. The drivers themselves were surprised by their consistent use of this point. Figure 2*a* shows the relative numbers of fixations in the regions around the tangent points. The distributions are centred within a degree of the tangent point itself on both left and right bends. As with straight driving (centre), they are elongated horizontally, with roughly exponential decline from the central peak. The time distribution of these fixations is shown in Fig. 2*b*. Gaze is directed to the tangent point, with a rather obvious saccade 1–2 s before the car enters each bend, and remains there with relatively few excursions for ~3 s into the bend. Half a second after the car has entered the bend, the gaze of all three drivers is directed to the tangent point for about 80% of the time (Fig. 2*b*). Clearly, the tangent point is visually important to the driver when steering into a turn.

Why should this be so? A likely answer is that tangent point direction (θ) relative to the car's heading is a very good predictor of the curvature of the road ahead[2]. It is easy to show that the curvature of the road between the car and tangent point is related to θ by

$$C = 1/(d\cos\theta) - 1/d \qquad (1)$$

where the curvature C is the reciprocal of the local inner radius of the road, and d is the lateral distance of the driver from the kerb. If d can be maintained by using some independent measurement, for example the perspective angle made by the kerb or lane marking near the car, then C is easily obtained from θ. And as the steering-wheel angle is directly proportional to C, equation (1) provides a simple steering strategy. In other schemes, the relative motion of the tangent point ($d\theta/dt$) can be used either to remove the need to compute d separately[2] or to monitor departures from a predicted constant curvature path[9]. Such predictions might come from the overall velocity flow field, which can specify the car's heading around a curve[10].

On a narrow undulating road, the tangent point is almost the only reliable cue to curvature because, unlike the general shape of the road ahead, it is unaffected by slope changes[11]. It is possible to steer while deliberately looking at the opposite side of the road, but it feels wrong, and one has to drive more slowly. Here as in other tasks[12], the brain prefers a 'do it where you look' strategy, in which the object guiding a control strategy is placed close to the centre of vision. In more relaxed wide-road driving, much more time is spent on tasks irrelevant to steering, which is why the importance of the tangent point has not previously become apparent[3]. The performance of driver J.C. (Fig. 1) shows that steering control can 'time-share' with other activities. In urban driving, where one may be called upon simultaneously to steer a course, avoid other vehicles and look for a street name, this capacity for dividing time while avoiding crosstalk between tasks is crucial. □

Received 24 March; accepted 20 May 1994.

1. Riemersma, J. B. J. in *Vision in Vehicles III* (ed. Gale, A. G.) 163–170 (North-Holland, Amsterdan, 1991).
2. Raviv, D. & Herman, M. in *Proc. IEEE Workshop on Visual Motion, Princeton, NJ* 217–225 (1991).
3. Serafin, C. *Univ. Michigan Transportation Res. Lab. Document* UMTRI–93–29 1–63 (1993).
4. Okuno, A., Fujita, K. & Kutami, A. in *Vision-based Vehicle Guidance* (ed. Masaki, I.) 222–237 (Springer, New York, 1992).
5. Dickmanns, E. D. *et al.* in *Proc. IEEE 4th Intl. Conf. on Computer Vision, Berlin* 608–615 (1993).
6. Land, M. F. *Nature* **359,** 318–320 (1992).
7. Land, M. F. in *Proc. IEEE Systems, Man and Cybernetics Conf., Le Touquet 1993* Vol. 3, 490–494 (1993).
8. Carpenter, R. H. S. *Movements of the Eyes* (Pion, London, 1988).
9. Lee, D. N. & Lishman, J. R. *Scand. J. Psychol.* **18,** 224–230 (1977).
10. Warren, W. H. Jr, Mestre, D. R., Blackwell, A. W. & Marris, M. W. *J. exp. Psychol.* **17,** 28–43 (1991).
11. Landwehr, K. in. *Vision in Vehicles III* (ed. Gale, A. G.) 187–194 North-Holland, Amsterdam, 1991).
12. Ballard, D. H., Hayhoe, M. M., Li, F. & Whitehead, S. D. *Phil. Trans. R. Soc.* B**337,** 331–339 (1992).

ACKNOWLEDGEMENTS. We thank R. Wakeling of Ford UK for arranging the loan of the car, Y. Coello and J. Horwood for technical help, J. Cuthbert and A. Marshall for driving the car (the third driver was M.F.L.), and T. Collett for reading and commenting on the manuscript. This study was supported in part by a grant from the Joint Council Initiative on Cognitive Science and Human Computer Interaction, and by an SERC grant to the Sussex Centre for Neuroscience.

Glutamate-mediated astrocyte–neuron signalling

Vladimir Parpura*†, Trent A. Basarsky*†, Fang Liu†‡, Ksenija Jeftinija†‡, Srdija Jeftinija†‡ & Philip G. Haydon*†§

* Department of Zoology and Genetics, † Neuroscience Program, or
‡ Department of Veterinary Anatomy, Iowa State University,
339 Science II, Ames, Iowa 50011, USA
§ To whom correspondence should be addressed

NEUROTRANSMITTER released from neurons is known to signal to neighbouring neurons and glia[1–3]. Here we demonstrate an additional signalling pathway in which glutamate is released from astrocytes and causes an NMDA (*N*-methyl-D-aspartate) receptor-mediated increase in neuronal calcium. Internal calcium was elevated and glutamate release stimulated by application of the neuroligand bradykinin to cultured astrocytes. Elevation of astrocyte internal calcium was also sufficient to induce glutamate release. To determine whether this released glutamate signals to neurons, we studied astrocyte–neuron co-cultures. Bradykinin significantly increased calcium levels in neurons co-cultured with astrocytes, but not in solitary neurons. The glutamate receptor antagonists D-2-amino-5-phosphonopentanoic acid and D-glutamylglycine prevented bradykinin-induced neuronal calcium elevation. When single astrocytes were directly stimulated to increase internal calcium and release glutamate, calcium levels of adjacent neurons were increased; this increase could be blocked by D-glutamylglycine. Thus, astrocytes regulate neuronal calcium levels through the calcium-dependent release of glutamate.

The release of glutamate from neuron-free cultures of neocortical astrocytes was monitored using high-performance liquid chromatography (HPLC). The neuroligand bradykinin (100 nM) increased glutamate in the superfusate ($n=16$; $P<0.02$, paired t-test; Fig. 1*a*). To investigate whether internal calcium concentration ($[Ca^{2+}]_i$) influences glutamate release from astrocytes, we monitored internal calcium using Fura-2 and found that bradykinin elevated astrocyte calcium concentration from 99 ± 10 to 568 ± 89 nM (mean ± s.e.m., $n=20$; Fig. 2). We used the calcium ionophore ionomycin to determine whether elevated internal calcium is sufficient to stimulate glutamate release. Addition of ionomycin (5 μM) in the presence of external calcium, but not in its absence, stimulated release of glutamate from astrocytes (Fig. 1*b*). Furthermore, bradykinin did not cause significant glutamate release when calcium was removed from the external saline ($P>0.1$, paired t-test). These results show that bradykinin induces the release of glutamate from neocortical astrocytes and that elevated internal calcium can induce glutamate release.

The role of glutamate transporters as mediators of bradykinin-induced glutamate release was investigated using glutamate transport inhibitors. Consistent with previous observations[4,5], *p*-chloromercuriphenylsulphonic acid (*p*-CMPS; 50 μM) and L-*trans*-pyrrolidine-2,4-dicarboxylate (PDC; 100 μM–1 mM) raised the basal level of glutamate in the astrocyte superfusate ($P<0.02$, Mann–Whitney U-test[6]). Furthermore, neither

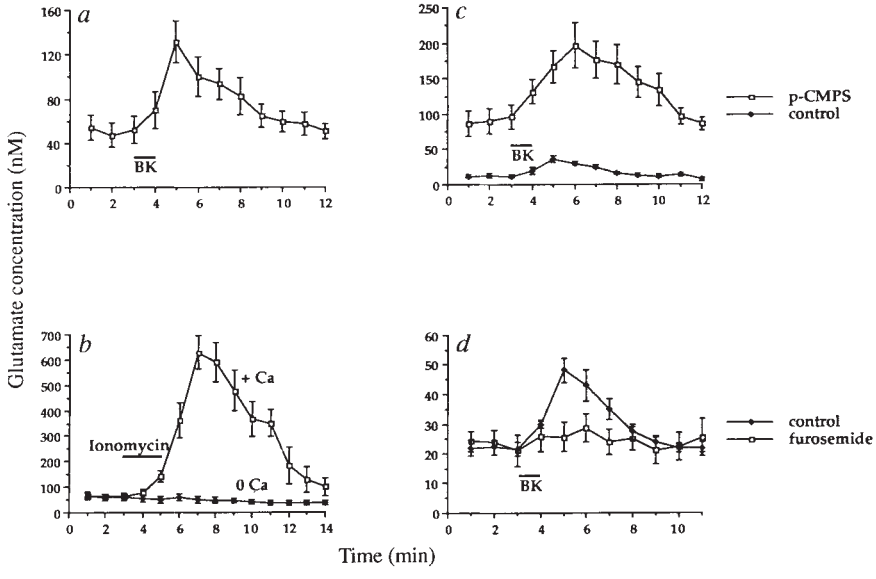

FIG. 1 Bradykinin causes calcium-dependent release of glutamate from astrocytes. The superfusate from astrocyte cultures was collected at 1-min intervals and levels of glutamate were measured using HPLC. *a*, Bradykinin (100 nM) increases glutamate release from astrocytes ($n=4$). *b*, Ionomycin (5 μM) stimulates glutamate release in cultures in calcium-containing saline (+Ca, $n=6$), but not in its absence (0 Ca; $n=7$). *c*, The glutamate-transport inhibitor *p*-CMPS (50 μM) raised the basal level of glutamate and enhanced the bradykinin-induced elevation of glutamate in superfusate ($n=6$), presumably as a result of inhibition of glutamate uptake. *d*, Furosemide (5 mM) blocks bradykinin-induced release of glutamate ($n=4$) without significantly affecting bradykinin-induced astrocyte calcium mobilization.
METHODS. Cultures from 1–4-day-old Sprague–Dawley rat cortices were enriched in type-1 astrocytes according to ref. 25 and were maintained in α-MEM medium. These cultures were neuron-free, as revealed by immunocytochemistry using an antibody directed against the synaptic protein synaptotagmin (1:250; clone 41.1, provided by R. Jahn). The amino-acid content of samples was determined by HPLC with fluorescence detection. Before injection, aliquots of samples were derivatized with *o*-phthalic aldehyde (OPA) 2-mercaptoethanol reagent (Pierce). Chromatography was performed on a 15 cm Microsorb-MV HPLC column (Rainin Instrument Co.) using a sodium acetate (pH 5.9)–methanol gradient. Points represent mean ± s.e.m. Solutions: A modified Ringer's solution used for perfusion contained (in mM): NaCl 128, KCl 1.9, KH_2PO_4 1.2, $CaCl_2$ 2.4, $MgSO_4$ 1.3, $NaHCO_3$ 26, and glucose 10 (pH = 7.4). In 'zero Ca' solution, calcium was replaced by 1 mM EGTA, 2.5 mM $MgSO_4$, 0.2 mM $CaCl_2$ to yield 24 nM free calcium.